

The Study of Capacitance Change during Electrolyte Penetration through Carbon-Supported Hydrous Ruthenium Oxide Prepared by the Sol-Gel Procedure*

V. V. Panić,^{a,**} A. B. Dekanski,^a V. B. Mišković-Stanković,^b and B. Ž. Nikolić^b

^aInstitute of Chemistry, Technology and Metallurgy, University of Belgrade, Njegoševa 12, 11001 Belgrade, Serbia

^bFaculty of Technology and Metallurgy, University of Belgrade, Karnegijeva 4, 11120 Belgrade, Serbia

Original scientific paper

Received: July 4, 2008

Accepted: August 26, 2008

The changes in capacitive behavior of C/H_xRuO_y composite material prepared by impregnating the Vulcan[®] XC 72R carbon black with oxide sols of different particle size are investigated as the electrolyte penetrates through the thin layer of the Nafion[®]-covered composite. The techniques of cyclic voltammetry and electrochemical impedance spectroscopy are used. Results of the investigation reveal the influence of potential cycling and the exposure time to the electrolyte on registered capacitive characteristics of composite. The cycling in a wide potential range causes the decrease in energy storage ability which depends on oxide particle size. Impedance measurements, however, show that the ability initially decreases and subsequently increases during exposure to the electrolyte as the consequence of the presence of Nafion[®] top-layer. Due to wettability and resistance issues, Nafion[®] top-layer can affect the pseudo-capacitive characteristics, and the energy storage ability of the composite consequently decreases.

Key words:

Electrochemical supercapacitors, pseudocapacitance, C/RuO_2 composites, charging/discharging processes, sol-gel procedure, electrochemical impedance spectroscopy

Introduction

Noble metal oxides of metallic conductivity exhibit almost pure capacitive characteristics in acid solutions within a wide potential range. Among them, the hydrous oxide of ruthenium, H_xRuO_y , is a widely investigated example.^{1–4} The capacitance values registered for powdered H_xRuO_y are considerably higher^{5,6} in comparison to so-called double-layer electrochemical capacitors, e.g., nano-processed carbons,⁷ since H_xRuO_y capacitive behavior involves remarkable pseudocapacitive contribution originating from surface solid state redox transition of ruthenium assisted by proton injection-ejection.^{1–3} The extent of pseudocapacitive contribution strongly depends on the ratio of the degrees of oxide hydration and crystallinity,⁵ which can be controlled by the conditions in the thermal treatment of the oxide.^{7,8}

Noble metal oxide-based supercapacitors, known after their good electrochemical properties for many applications,^{9–11} usually consist of a powdered carbon material in the form of blacks, nanotubes and nanofibres, impregnated by differently prepared oxide.^{6,7,12–16} The capacitive characteristics of this

kind of supercapacitive composite comprise the double layer capacitance of the carbon material and oxide pseudocapacitance.

The preparation of ruthenium oxide-based supercapacitive materials usually involves oxide precipitation from a solution of ruthenium salts containing suspended carbon powder.^{5,6} In previous work,^{7,17–19} the C/H_xRuO_y composite was prepared from the oxide sol prepared by forced hydrolysis of $RuCl_3$. The carbon black was impregnated by mixing the water suspension of carbon black with the oxide sols of different ageing times. The capacitive properties of oxide-impregnated high surface area carbon black (Black Pearls 2000[®] (BP), BET surface area:⁹ 1745 m² g⁻¹) were found to be dependent on the temperature of thermal treatment, the oxide concentration in the impregnating medium, and the ageing time of oxide sol.^{7,17} Due to high surface area of carbon black, the availability of active surface of the composite is limited to rather slow charging/discharging process. Less pronounced dependence of capacitive performances of the composite on the properties of oxide sol and impregnating conditions was registered when carbon black of considerably lower surface area (Vulcan[®] XC 72R (XC), BET surface area:⁹ 248 m² g⁻¹) was impregnated.¹⁸ However, the capacitive ability of XC-impregnated composite decreased with the number of charging/discharging cycles during cyclic

*Partially presented as Keynote Lecture at the First Regional Symposium on Electrochemistry of South-East Europe, Rovinj, Croatia, May 4–8, 2008.

**Corresponding author: panic@ihtm.bg.ac.yu

voltammetry. The extent of the decrease, which was found to be different for charging and discharging half-cycle, was dependent on the ageing time of oxide sol (*i.e.*, oxide particle size).¹⁸ In the paper dealing with XC-impregnated composite¹⁸ the decrease was tentatively assigned to the oxide depletion from the carbon surface due to relatively weak adhesion of the impregnating oxide to the carbon black support. However, the additional effect related to the wettability of XC, known after its hydrophobic surface contrary to BP, which can affect the electrolyte penetration into the composite electrode layer, was not taken into the consideration.^{20,21} Furthermore, common preparation procedure of a thin layer of the carbon-supported electrocatalyst involves the application of Nafion[®] as top-layer, which ensures the adhesion of the composite layer to the current connector beneath.^{22,23} Nafion[®] membrane is used as separator in real supercapacitor devices and affects one of its main characteristics – internal resistance.¹ In previous work, Nafion[®] was applied from dilute water solution over dried composite or XC layer and evaporated at room temperature.¹⁸ By the immersion of the electrode assembly into the electrolyte the phase boundary was visually observed, which needed several hours to disappear. This wetting time was shorter if the electrode was subjected to cyclic voltammetry. The wettability of carbon surface can also influence the properties of Nafion[®] top-layer (or separator/electrode interphase), which could hinder additionally the electrolyte penetration.

In order to analyze whether the loss of capacitive ability of XC-supported composite is related to the oxide depletion effect or poor wettability, and to obtain detailed insight of the role of Nafion[®], capacitive properties of a thin porous composite layer is investigated in this paper. The effect of the time of exposure to the electrolyte and the influence of the number of charging/discharging cycles, cyclic conditioning and the presence of Nafion[®] top-layer on the composite characteristics was investigated by cyclic voltammetry (CV) and electrochemical impedance spectroscopy (EIS).

Experimental

Oxide sol

Colloidal dispersion of ruthenium oxide was prepared by forced hydrolysis of 5.0 g RuCl₃ (RuCl₃ · xH₂O dried at 120 °C for 24 h in nitrogen atmosphere) in 0.27 mol dm⁻³ HCl at boiling temperature,¹⁹ which should give the concentration of the solid phase of about 0.65 mass % in the resulting oxide sol, calculated to RuO₂. The starting solution was aged for 2.5, 24 and 46 h (ageing time, t_{ag} ,

the duration of the forced hydrolysis process). The final concentration of the solid phase for all ageing times was found to be around 1.0 mass % (dry residue treated in air at 120 °C for 24 h), which indicates the presence of highly hydrated oxide.⁷

Impregnation of carbon black support

The XC/H_xRuO_y composite is obtained by impregnation of a carbon black support using ultrasonic agitation of a mixture of oxide sol and carbon black suspension (carbon to hydrous oxide ratio was set to 3.4 : 1.0 w/w). The carbon black suspension was previously prepared in 0.27 mol dm⁻³ HCl. The commercially available Vulcan[®] XC-72 R (Cabot Corp., Canada) was used as the carbon black support. The concentration of the oxide solid phase in the impregnating medium was 8.8 g dm⁻³. After separation from the impregnating medium, prepared XC/H_xRuO_y composites, XC/R2.5, XC/R24 and XC/R46, were dried in air at 120 °C for 24 h.

Electrode assembly

The dried composite was ultrasonically suspended in water (3.0 mg mL⁻¹), and the suspension was applied onto an Au disc as current collector (7 mm in diameter), which gave 59.2 µg cm⁻² of the composite layer. After drying in air at room temperature, the formed composite layer was covered by Nafion[®] from 10 : 1 (v/v) mixture of water and commercial Nafion[®] alcoholic solution (5 mass %, 1100 E.W., Aldrich) to ensure the adhesion of the composite layer to the Au current collector. However, if the composite layer is dried at 60 °C for 30 min and handled carefully, the adhesion is good enough to allow experiments without Nafion[®] top-layer. This opportunity was used to investigate the influence of Nafion[®] top-layer on the capacitive properties of XC/R46 composite by electrochemical impedance spectroscopy.

In order to compare the properties of prepared electrode composite layer and XC support, the electrode layer of XC was treated under the same conditions.

Measurements

The Nafion[®]-covered composite layers (and one uncovered in the case of XC/R46 composite) onto Au served as the working electrode in a cell equipped with a Pt mesh as the counter electrode and saturated calomel electrode (SCE) as the reference electrode. The CV and EIS measurements were done in oxygen-free 1.0 mol dm⁻³ H₂SO₄ at room temperature, using voltammograph CV-27, Bioanalytical Systems Inc., UK, and FAS2 Femtostat Potentiostat/Galvanostat, Gamry Instruments, USA. The EIS measurements were performed around the

potential of $0.50 V_{SCE}$ with amplitude of 5 mV. In order to follow the changes in capacitive properties due to electrochemical pretreatment, the EIS spectra were recorded before and after single-frequency cyclic conditioning (SFCC) which is done for 75 cycles around the potential of $0.250 V_{SCE}$ with amplitude of 0.355 V at frequency of 0.010 Hz. The SFCC conditions are equivalent to that of CV at the scan rate of $20 mV s^{-1}$ which is used to examine the changes in voltammetric response upon cycling.

Having in mind that composite characteristics change with exposure time, EIS measurements were done in the direction from high to low frequencies with 7 points per decade and Gamry Femtostat operating in fast mode for data collection. The stability of fast mode Lissajou figures (one figure per frequency) was checked at lower frequencies by comparison of the figures recorded at normal operation mode (at least two figures per frequency), which defined the lowest accurate frequency for every single composite layer. Additionally, the data collected in the half of the last frequency decade were considered as less accurate in the fitting procedure.

The EIS data were fitted by ZView[®] software, Scribner Associates Inc., Southern Pines, NC, USA, through 100 iterations. The goodness of fit was judged towards weighted sum of squares to be below 0.020 and the data-modulus type of weighting. The relative error of all parameter values was below 20 %.

Results and discussion

Since the origin of wettability issue is related to the XC support, the changes in the CV characteristics of Nafion[®]-covered thin electrode layer of XC support was investigated by cycling from the moment of electrode immersion into the electrolyte. The cyclic voltammograms registered immediately after immersion and after 30 and 375 min of cycling are shown in Fig. 1a. The voltammograms are of usual shape for carbon materials, with the weak appearance of redox pair around $0.30 V_{SCE}$ which is related to the oxygen-containing functional groups at carbon surface.^{24–26} The voltammetric currents increase with cycling and exposure time. The increase is similar for charging and discharging half-cycles. Corresponding change in the anodic capacitance upon cycling is given in Fig. 1b. The largest increase in capacitance is registered during the first 30 cycles, while between the 100th and 250th cycle the increase is negligible. An additional near 30 %-increase is observed between the 250th and 400th cycle, after which the capacitance reaches a plateau at $12 F g^{-1}$. By comparing the capacitance values with the pub-

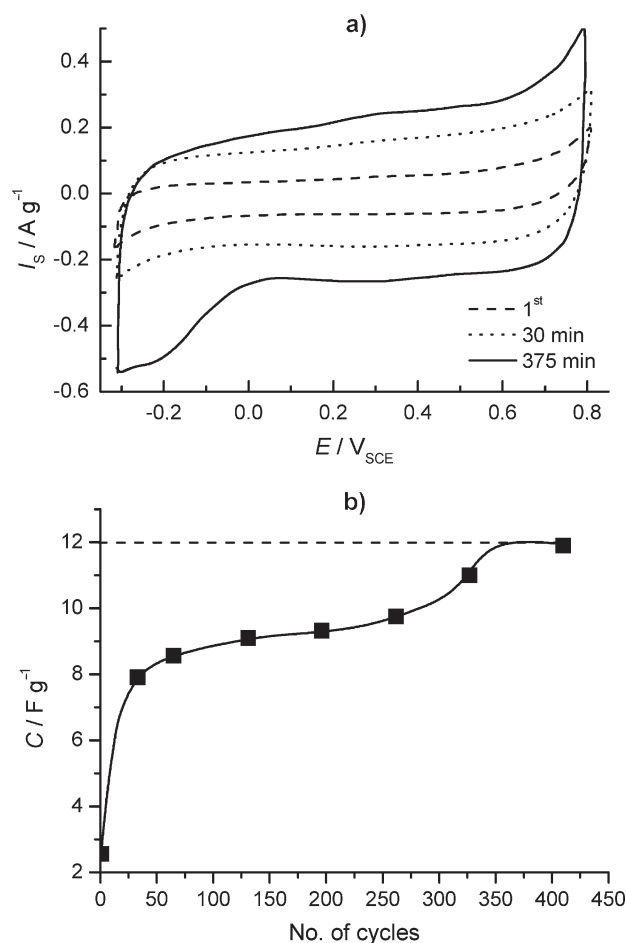


Fig. 1 – a) Cyclic voltammograms of Nafion[®]-covered thin XC layer registered during exposure to the electrolyte, and b) dependence of the anodic voltammetric capacitance of Nafion[®]-covered thin XC layer on the number of CV cycles. Electrolyte: deaerated $1.0 mol dm^{-3} H_2SO_4$; sweep rate: $20 mV s^{-1}$.

lished data of in-depth capacitance profile of the XC layer prepared without Nafion[®],²⁷ it can be concluded that the capacitance in the 1st cycle, ($2.5 F g^{-1}$), is similar to that related to the Nafion[®]-uncovered XC layer surface facing directly the bulk of the electrolyte, found to be $\sim 2 F g^{-1}$.²⁷ This indicates that only the outer surface of XC layer in contact with the conductive Nafion[®] top-layer is involved in the voltammetric response of the 1st cycle. During the 1st cycle, the electrolyte does not have time to wet the electrode assembly but only the surface of Nafion[®] top-layer, and hence the inner surface of the XC layer is isolated. As the Nafion[®] top-layer becomes wet during the first 30 cycles, the electrolyte starts to penetrate towards XC beneath and the capacitance sharply increases. At the end of Nafion[®] wetting ($\sim 75^{th}$ cycle) the capacitance reaches the value of $\sim 8.5 F g^{-1}$ and then slowly increases to $\sim 9.5 F g^{-1}$ (250th cycle). At this stage, the electrolyte starts to penetrate the XC layer and an increasing part of the layer's inner sur-

face begins to be involved in the voltammetric response. During the cycling in this stage the concentration of oxygen-containing functional groups at the surface of carbon particles is increasing, which produces moderate increase of the capacitance. Finally, after 400th cycle, the pores of XC layer is filled by electrolyte, the highest concentration of oxygen-containing functional groups is achieved and the capacitance reaches the plateau of 12 F g⁻¹. This value corresponds to the highest value for the outer surface of XC layer prepared without Nafion[®] which can be achieved under given charging/discharging conditions.²⁷

Contrary to the CV charging/discharging characteristics of Nafion[®]-covered XC layer, which exhibit considerable increase in the capacitance upon cycling, the XC/H_xRuO_y composite layers suffer from the loss of energy storage ability upon cycling, as concluded in the previous paper.¹⁸ The CV behavior upon cycling of XC/R2.5 and XC/R46 composite layer is presented in Fig. 2. It is seen that the voltammetric currents decrease upon cycling, in different degree depending on the oxide sol ageing time. The decrease was less pronounced for the composite prepared from oxide sol, aged longer. Additionally, it can be concluded that there is no decrease of the voltammetric currents for XC/R46 composite layer after *ca.* 80 cycles, while the decrease continues for XC/R2.5 composite layer beyond the 200th cycle. This behavior is clearly envisaged from the dependences of anodic and cathodic voltammetric capacitance on cycling, shown in Fig. 3. Both anodic and cathodic voltammetric capacitance decrease sharply in the first few cycles and

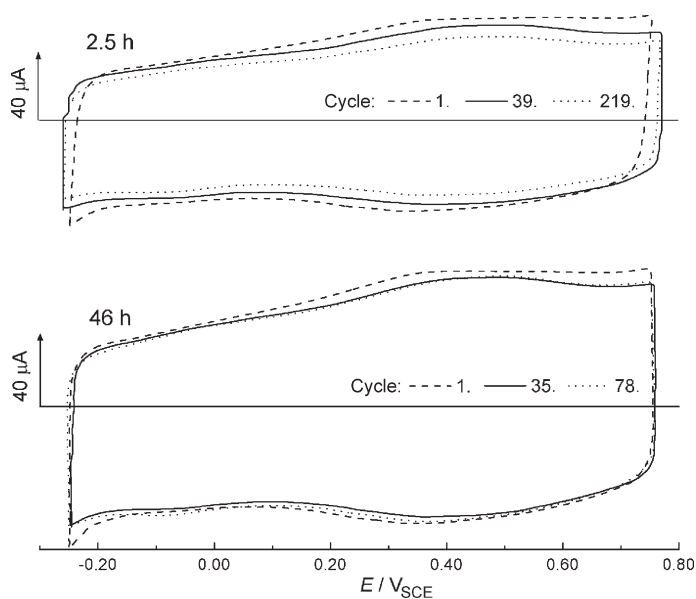


Fig. 2 – Cyclic voltammograms of the Nafion[®]-covered XC/H_xRuO_y composites prepared from oxide sols of indicated ageing times after given number of cycles. Electrolyte: deaerated 1.0 mol dm⁻³ H₂SO₄; sweep rate: 20 mV s⁻¹.

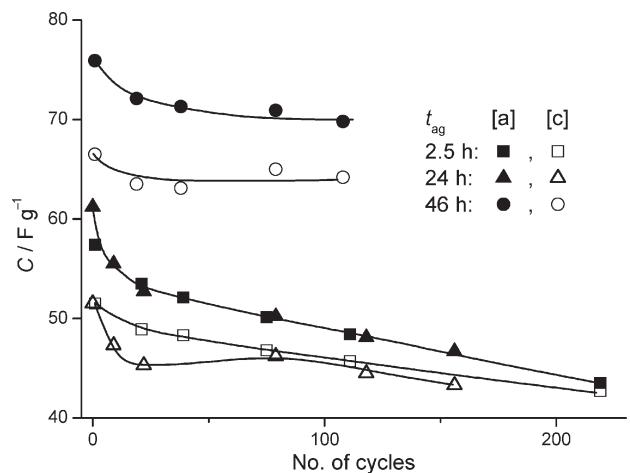


Fig. 3 – Changes of anodic ([a]) and cathodic ([c]) voltammetric capacitances of XC/H_xRuO_y composites, prepared from oxide sols aged for indicated times, as the functions of CV cycles

afterwards behave differently depending on the ageing time of oxide sol. For the longest ageing time (46 h), the capacitance becomes stable with cycling; for 2.5 and 24 h it continues to decrease. Another important feature of capacitive characteristics of prepared composites (Fig. 3) is that the discharging ability of longer aged composites (24 and 46 h) is always lower than the charging one. For short ageing time (2.5 h) this difference continuously decreases with cycling, and finally, the CV profile of XC/R2.5 composite becomes fully symmetric after *ca.* 230 cycles. The difference between charging and discharging capacitance, and the dependences on cycling indicate that the oxide pseudocapacitive characteristics modify during the cycling, tending to be reversible. It appears that the longer the ageing time (*i.e.*, larger oxide particles) the longer cycling will be required for the reversibility to be achieved.

More detailed analysis of the changes in composite capacitive characteristics may be obtained from the impedance measurements. Capacitance complex plane presentations for Nafion[®]-covered composites registered at open circuit potential upon electrode immersion into the electrolyte and after single-frequency cycling conditioning are shown in Fig. 4. In all cases, the capacitive loops are registered at higher frequencies, followed by different types of tails in the low-frequency domain. The most pronounced differences between the EIS spectra registered before and after conditioning are seen for XC/R2.5 composite layer. The main difference for XC/R2.5 and XC/R46 composite layer caused by conditioning is the diminishing of the real part of capacitance, while for XC/R24 composite layer the change is mainly related to the imaginary part. Contrary to the cases of XC/R2.5 and XC/R46 composite layer, for which the decrease of the real

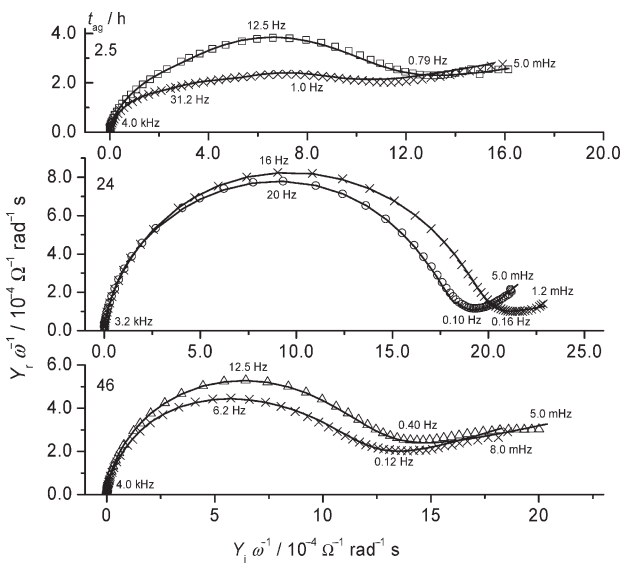


Fig. 4 – Capacitance complex plane plots for the composites prepared from oxide sols aged for indicated times, registered at open circuit potential before (\square , \circ , \triangle) and after (\times) single-frequency cycling conditioning. Lines illustrate the impedance data of equivalent electrical circuits.

part is registered upon conditioning, the imaginary capacitance of XC/R24 composite layer increases upon conditioning.

In order to quantify the impedance characteristics shown in Fig. 4 the fitting procedure involving transmission line model of equivalent electrical circuit (EEC)^{1,28,29} was applied. Having in mind the criteria mentioned in the Experimental section, the EECs that gave the best-fit results of experimental EIS data are given in Fig. 5. For all investigated samples 4-branch EEC was required for good fitting (Fig. 5b), except SFCC conditioned XC/R2.5 composite layer (Fig. 5a), for which 3-branch EEC showed the best fitting results. The difference in 4-branch EECs for investigated samples was whether or not some of the constant phase elements

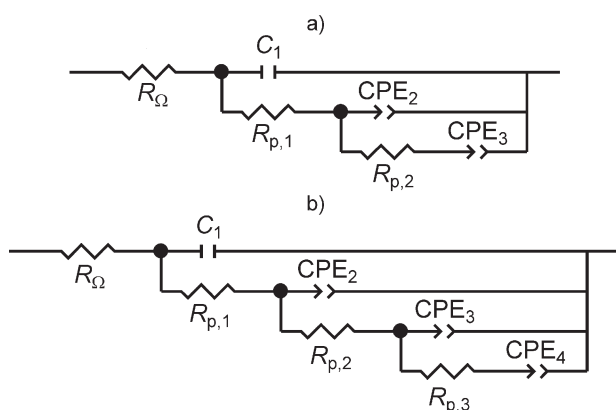


Fig. 5 – Equivalent electrical circuits used to fit EIS data of a) XC/R2.5 composite layer after single-frequency cycling conditioning and b) all other cases

(CPE)³⁰ are replaced by pure capacitors (C), although at least one CPE was required, as it is shown by circuit notation given in Table 1. The values of the α parameter³⁰ of all CPEs were in the range 0.73–0.98, pointing out the inhomogeneity of corresponding surface and introducing the corresponding admittance suitable for the calculation of related capacitance values according to the well-known procedure.^{30,31}

The resistance R_Ω relates to the ohmic resistance of the bulk electrolyte, while the resistances $R_{p,i}$ ($i = 1, 2, 3$) represent the pore resistances of the layer (ohmic resistances of the electrolyte in the pores). The capacitance C_1 relates to the capacitive response of the outer surface of the layer, which directly faces the electrolyte bulk, and the capacitances C_i ($i = 2, 3, 4$) correspond to the inner surface of the layer, accessible through the pores. It can be assumed that each separate series combination $R_{p,i}C_i$ corresponds to the impedance characteristics of the coating at a distance z_i from the coating surface ($z = 0$) towards the bottom of the pore.¹

Having in mind the presence of hardly-wettable Nafion[®] top-layer, the elements $R_{p,i}$ and C_i should change their reference from Nafion[®] top-layer towards the composite layer beneath (characterized by the instant penetration depth) as the exposure time of the conditioned/unconditioned electrode assembly increases.

This can be envisaged from the values of the EEC parameters given in Table 1. Looking at the values of total capacitance gained ($\sum_{n=1}^4 C_n$) it can be observed that in the case of larger oxide particles (XC/R24 and XC/R46) similar values are registered before and after SFCC, while in the case of small particles (XC/R2.5) the increase was registered as the consequence of SFCC. For all samples, the values are lower than those registered by CV upon cycling (Fig. 3), which is the consequence of the difference between cycling limits in CV and EIS amplitude. A much wider range of potential is applied in CV, which promotes the pseudocapacitive behavior, as pointed out in the previous work.²⁹ The values of total capacitance show also the dependence on the ageing time of oxide sols, with the lowest value obtained for XC/R2.5 and the highest for XC/R46, similar to the results reported and discussed earlier.¹⁸

The influence of SFCC on XC/R2.5 is reflected in the requirement to withdraw the last branch from EEC, which has been subjected to the high $R_{p,3}$ value in AI state. As the electrolyte wets and penetrates the assembly during the SFCC, the preceding pore resistance values ($R_{p,1}$ and $R_{p,2}$) decrease, while the capacitances in corresponding branches dou-

Table 1 – Values of pore resistances, $R_{p,n}/\Omega$, and capacitances, $C_n/F\ g^{-1}$, obtained by fitting the EIS data of XC/RuO_x composites, in the function of ageing time of oxide sol, t_{ag} , and pretreatment of composite electrode layer (AI – after immersion; SFCC – single-frequency cyclic conditioning)

t_{ag}/h		Circuit notation	$R_{p,1}$	$R_{p,2}$	$R_{p,3}$	C_1	C_2	C_3	C_4	$\sum_{n=1}^4 C_n$
2.5	AI	$R_{\Omega}(R_{p,1}(R_{p,2}(R_{p,3}CPE_4)CPE_3)CPE_2)C_1$	4.3	38	380	3.6	3.5	4.0	3.4	14.5
	SFCC	$R_{\Omega}(R_{p,1}(R_{p,2}CPE_3)CPE_2)C_1$	3.6	24.7	–	4.8	6.4	7.8	–	19
24	AI	$R_{\Omega}(R_{p,1}(R_{p,2}(R_{p,3}CPE_4)C_3)C_2)C_1$	1.2	4.8	43.7	9.2	16.4	10.7	4.7	41
	SFCC	$R_{\Omega}(R_{p,1}(R_{p,2}(R_{p,3}C_4)CPE_3)CPE_2)C_1$	1.5	16.0	280	11.2	18.6	7.3	2.1	39.2
46	AI	$R_{\Omega}(R_{p,1}(R_{p,2}(R_{p,3}CPE_4)C_3)C_2)C_1$	2.8	10.7	86.8	4.8	6.0	8.0	5.5	24.3
	SFCC	$R_{\Omega}(R_{p,1}(R_{p,2}(R_{p,3}C_4)CPE_3)CPE_2)C_1$	1.8	4.9	315	5.6	6.8	9.4	0.87	22.7

bles. This means that, as the penetration depth increases, the active inner surface is continuously “transferred” to the EEC high-frequency branches (closer to the electrolyte bulk and R_{Ω}), and additionally, wetted Nafion® top-layer is of lower resistance at the pore orifice in SFCC assembly state with respect to its dry AI state.

Apparently, the changes in the physical state of XC/R24 and XC/R46 electrode assemblies during the SFCC may be ascribed to the increase in penetration depth as the Nafion® top-layer becomes wet. The pore resistances of XC/R24 increase during SFCC, which becomes more pronounced as the branch is of higher order (2nd to 4th, located farther from R_{Ω} and the 1st branch). Consequently, the capacitances in the branches containing pore resistances subjected to the highest increase caused by SFCC (3rd and 4th branch) decreased with respect to the AI state. Negligible increase in capacitance is registered in the 1st and 2nd branch.

If the composite is prepared with largest oxide particles (XC/R46), the considerable increase in pore resistance is observed only in, last, 4th branch of EEC ($R_{p,3}$), followed by the pronounced decrease in corresponding capacitance (C_4).

In order to gain more information about the registered strange behavior of XC/R24 and XC/R46 electrode assemblies, the XC/46 assembly was left in contact with electrolyte for 24 h at open circuit potential before EIS experiments with SFCC. Additionally, the behavior of XC/R46 composite layer without Nafion® top-layer was checked in the same way as in the experiments the data of which are shown in Table 1. The capacitance complex plane plots of these experiments are shown in Fig. 6, while the obtained fitting results are given in Table 2. It is seen from Fig. 6 that capacitive ability increases with prolonged contact with electrolyte, while considerably higher capacitance is registered for the composite without Nafion® top-layer.

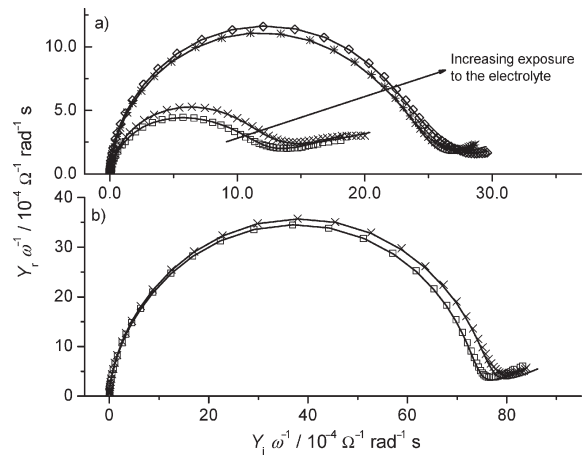


Fig. 6 – Capacitance complex plane plots for the XC/R46 composite prepared with (a) and without (b) Nafion® top-layer, registered at open circuit potential before (×, ◇) and after (□, ×) single-frequency cyclic conditioning. Lines illustrate the impedance data of equivalent electrical circuits.

Table 2 – Influence of the single-frequency cyclic conditioning (SFCC) on the pore resistances, $R_{p,n}/\Omega$, and capacitances, $C_n/F\ g^{-1}$, of XC/R46 composite electrode layer with and without Nafion® top-layer. The composite electrode layer prepared with Nafion® was in contact with the electrolyte for 24 h after the experiments related to Table 1. Circuit notation: $R_{\Omega}(R_{p,1}(R_{p,2}(R_{p,3}CPE_4)C_3)C_2)C_1$.

Circuit parameter	With Nafion		Without Nafion	
	before SFCC	after SFCC	before SFCC	after SFCC
$R_{p,1}$	1.9	1.5	0.84	0.89
$R_{p,2}$	36.8	15.4	4.6	5.0
$R_{p,3}$	840	229	135	220
C_1	19.4	19.6	48.2	56.9
C_2	24.6	21.3	66.6	66.7
C_3	7.7	8.4	38.8	35.4
C_4	5.1	4.2	3.6	4.9
$\sum_{n=1}^4 C_n$	56.8	53.5	157.2	163.9

As the consequence of 24 h-contact with electrolyte, total capacitance of XC/R46, $\sum_{n=1}^4 C_n$ (Table 2), doubles with respect to the data registered after the immersion (Table 1). The pore resistances in branches far from R_{Ω} ($R_{p,1}$ and $R_{p,2}$) are considerably higher, but also the capacitance values of the outer layer parts (C_1 and C_2). However, the capacitances related to the deep layer surface (C_3 and C_4) are quite similar to the case of just immersed electrode assembly. As the consequence of SFCC, a negligible decrease in total capacitance is registered, but the pore resistances considerably decrease with the exposure time. On the other hand, if Nafion[®] top-layer is not present, total capacitance slightly increases, while the pore resistance of deep inner parts of the layer ($R_{p,3}$) increases considerably. This indicates that proton-assisted surface solid state redox processes of Ru are promoted by SFCC. Being fully developed, these processes become diffusion-controlled (increased $R_{p,3}$).

From the presented results and considerations it appears that the decrease in capacitive ability, registered by CV, can hardly be assigned to the oxide depletion, but to the “Nafion[®] effect”. Due to the Nafion[®] top-layer wettability issue, the pore resistance of the composite layer is rather large upon immersion into the electrolyte. As the electrode assembly is exposed to the electrolyte for a longer time, the wetting of a Nafion[®] top-layer causes pore resistance to decrease, as indicated by EIS measurements. This simultaneously hinders the full development of the pseudocapacitive characteristics of the ruthenium oxide, which may be put forward by SFCC. Even if the fully wetted state is achieved (at open circuit potential), only one-third of total energy storage ability (with fully developed pseudocapacitance) can be reached when Nafion[®] top-layer is present.

If the ageing time of applied oxide sol is taken into the consideration, it appears that Nafion[®]-covered composite layer made of smaller oxide particles (XC/R2.5) is wetted faster than that made of larger ones (XC/R24 and XC/R46). Generally, the capacitance initially decreases and subsequently increases during the wetting of the electrode assembly. This appears to be due to Nafion[®]-hindered promotion of oxide pseudocapacitance, since only increase is registered for XC (Fig. 1). The transition between decrease and increase of the capacitance is reached in shorter times if the oxide particles are smaller (for XC/R2.5 it happened during the experiments which data are shown in Table 1).

Conclusion

The cyclic voltammetry and impedance investigation of the capacitive characteristics of C/H_xRuO_y composite material in a form of Nafion[®]-covered thin layer showed the influence of Nafion[®] top-layer, which depends on the exposure time to the electrolyte and electrode cycling conditioning. As the electrode assembly is immersed into the electrolyte it starts to wet slowly, which causes pore resistance and capacitance to decrease, since wet Nafion[®] top-layer hinders the promotion of the oxide pseudocapacitive ability. By reaching the fully wetted state of the electrode assembly, the composite capacitance starts to increase as the electrolyte penetration depth increases. After prolonged exposure to the electrolyte, the composite achieves about one-third of the capacitive ability of the composite prepared without Nafion[®] top-layer. The final capacitive characteristics are developed more easily if the oxide particles are smaller, while longer exposure time is required for the composites prepared with larger oxide particles. This is because the wetting process is facilitated in the case of an electrode assembly with small particles.

ACKNOWLEDGEMENTS

The results presented in this paper were realized due to the financial support of the Ministry of Science and Technological Development of the Republic of Serbia, Projects No. 142048 and 142061.

References

1. Conway, B. E., *Electrochemical Supercapacitors – Scientific Fundamentals and Technological Applications*, Plenum Publishers, New York, 1999.
2. Trasatti, S., O’Grady, W., in *Gerisher, H., Tobias, C. W.* (Eds.), *Advances in Electrochemistry and Electrochemical Engineering*, Vol. 12, Wiley, New York, 1981.
3. Sugimoto, W., Kizaki, T., Yokoshima, K., Murakami, Y., Takasu, Y., *Electrochim. Acta* **49** (2004) 313.
4. Trasatti, S., in *Wieckowski, A.* (Ed.), *Interfacial Electrochemistry – Theory, Experiment and Applications*, Marcel Dekker Inc., New York, 1999, p. 769.
5. Zheng, J. P., Jow, T. R., *J. Electrochem Soc.* **142** (1995) L6.
6. Ramani, M., Haran, B., White, R., Popov, B., *J. Electrochem. Soc.* **148** (2001) A374.
7. Panić, V., Vidaković, T., Gojković, S., Dekanski, A., Nikolić, B., *Electrochim Acta* **48** (2003) 3805.
8. McKeown, D., Hagans, P., Carette, L., Russell, A., Swider, K., Rolison, D., *J. Phys. Chem. B* **103** (1999) 4825.
9. Kinoshita, K., *Carbon – Electrochemical and Physicochemical Properties*, Wiley, New York, 1988.

10. Terzić, S., Tripković, D., Jovanović, V. M., Tripković, A., Kowal, A., *J. Serb. Chem. Soc.* **72** (2007) 165.
11. Sabzi, R. E., Hasanzadeh, A., Ghasemlu, K., Heravi, P., *J. Serb. Chem. Soc.* **72** (2007) 993.
12. Cui, G., Zhi, L., Thomas, A., Lieberwirth, I., Kolb, U., Müllen, K., *Chem. Phys. Chem.* **8** (2007) 1013.
13. Lee, B. J., Sivakkumar, S. R., Ko, J. M., Kimb, J. H., Jo, S. M., Kim, D. Y., *J. Power Sources* **168** (2007) 546.
14. Reddy, A. L. M., Ramaprabhu, S., *J. Phys. Chem. C* **111** (2007) 7727.
15. Li, H., Wang, R., Cao, R., *Micropor. Mesopor. Mat.* **111** (2008) 32.
16. Pico, F., Ibañez, J., Lillo-Rodenas, M. A., Linares-Solano, A., Rojas, R. M., Amarilla, J. M., Rojo, J. M., *J. Power Sources* **176** (2008) 417.
17. Panić, V., Dekanski, A., Gojković, S., Mišković-Stanković, V., Nikolić, B., *Mater. Sci. Forum* **453-454** (2004) 133.
18. Panić, V., Dekanski, A., Gojković, S., Milonjić, S., Mišković-Stanković, V., Nikolić, B., *Mater. Sci. Forum* **494** (2005) 235.
19. Panić, V. V., Dekanski, A., Milonjić, S. K., Atanasoski, R. T., Nikolić, B., *Colloids Surfaces A* **157** (1999) 269.
20. Fang, B., Binder, L., *J. Electroanal. Chem.* **609** (2007) 99.
21. Panić, V. V., *J. Serb. Chem. Soc.* **73** (2008) 661.
22. Babić, B. M., Kaludjerović, B. V., Vračar, Lj. M., Radmilović, V., Krstajić, N. V., *J. Serb. Chem. Soc.* **72** (2007) 773.
23. Elezović, N. R., Babić, B. M., Vračar, Lj. M., Krstajić, N. V., *J. Serb. Chem. Soc.* **72** (2007) 699.
24. Dekanski, A., Stevanović, J., Stevanović, R., Nikolić, B. Ž., Jovanović, V. M., *Carbon* **39** (2001) 1195.
25. Maruyama, J., Abe, I., *Electrochim. Acta* **46** (2001) 3381.
26. Braun, A., Kohlbrecher, J., Bärtsch, M., Schnyder, B., Kötz, R., Haas, O., Wokaun, A., *Electrochim. Acta* **49** (2004) 1105.
27. Panić, V. V., Stevanović, R. M., Jovanović, V. M., Dekanski, A. B., *J. Power Sources* **181** (2008) 186.
28. Panić, V., Dekanski, A., Milonjić, S., Mišković-Stanković, V. B., Nikolić, B., *J. Serb. Chem. Soc.* **71** (2006) 1173.
29. Panić, V. V., Vidaković, T. R., Dekanski, A. B., Mišković-Stanković, V. B., Nikolić, B. Ž., *J. Electroanal. Chem.* **609** (2007) 120.
30. Johnson, D., ZView® Software help file, Scribner Associates Inc., ©1990–2002.
31. Jović, V. D., Jović, B. M., *J. Electroanal. Chem.* **541** (2003) 12.